"Raisin bread sign" feature of pontine autosomal dominant microangiopathy and leukoencephalopathy

Mai Kikumoto,[1,2,3] Takashi Kurashige,[4] Tomohiko Ohshita,[1,2,4] Kodai Kume,[3] Osamu Kikumoto,[5] Tomohisa Nezu,[1] Shiro Aoki,[1] Kazuhide Ochi,[2,6] Hiroyuki Morino,[1,7] Eiichi Nomura,[8] Hiroshi Yamashita,[2] Mayumi Kaneko,[9] Hirofumi Maruyama,[1] Hideshi Kawakami[3]

Abstract

Pontine autosomal dominant microangiopathy and leukoencephalopathy is one of hereditary cerebral small vessel diseases caused by pathogenic variants in *COL4A1* 3'UTR and characterized by multiple small infarctions in the pons. We attempted to establish radiological features of this disease.

We performed whole exome sequencing and Sanger sequencing in one family with undetermined familial small vessel disease, followed by clinicoradiological assessment and a postmortem examination. We subsequently investigated clinicoradiological features of patients in a juvenile cerebral vessel disease cohort and searched for radiological features similar to those found in the aforementioned family. Sanger sequencing was performed in selected cohort patients in order to detect variants in the same gene.

An identical variant in the *COL4A1* 3'UTR was observed in two patients with familial small vessel disease and the two selected patients, thereby confirming the pontine autosomal dominant microangiopathy and leukoencephalopathy diagnosis. Furthermore, postmortem examination showed that the distribution of thickened media tunica and hyalinized vessels was different from that in lacunar infarctions.

The appearance of characteristic multiple oval small infarctions in the pons, which resemble raisin bread, enable us to make a diagnosis of PADMAL. This feature, for which we coined the name "raisin bread sign", was also correlated to the pathological changes.

Author affiliations:

1 Department of Clinical Neuroscience and Therapeutics, Hiroshima University Graduate School of Biomedical and Health Sciences, Hiroshima 7348551, Japan

2 Department of Neurology, Hiroshima City North Medical Center Asa Citizens Hospital, Hiroshima 7310293, Japan

3 Department of Molecular Epidemiology, Research Institute for Radiation Biology and Medicine, Hiroshima University, Hiroshima 7348553, Japan

4 Department of Neurology, National Hospital Organization Kure Medical Center and Chugoku Cancer Center, Kure 7370023, Japan

5 Ideshita Clinic, Hiroshima 7391734, Japan

6 Department of Neurology, Hiroshima Prefectural Hospital, Hiroshima 7348530, Japan

7 Department of Medical Genetics, Tokushima University Graduate School of Biomedical Sciences, Tokushima 7708503, Japan

8 Department of Neurology, Hiroshima City Hiroshima Citizens Hospital, Hiroshima 7308518, Japan

9 Department of Diagnostic Pathology, Hiroshima City North Medical Center Asa Citizens Hospital, Hiroshima 7310293, Japan

Correspondence to: Takashi Kurashige

Department of Neurology

National Hospital Organization Kure Medical Center and Chugoku Cancer Center

Kure 7370023, Japan

E-mail: takashi-kurashige@hiroshima-u.ac.jp

Running title: "Raisin bread sign" feature of PADMAL

Keywords: PADMAL; *COL4A1*; hereditary stroke; MRI; cerebral small vessel disease and pons

Introduction

Over the last decades, several monogenic cerebral small vessel diseases (cSVD) have been reported, with the diagnostic value of some of the radiological features having been identified.[1-5] Pontine autosomal dominant microangiopathy and leukoencephalopathy (PADMAL) is one of the hereditary cSVD that is caused by pathogenic variants in the *COL4A1* 3' untranslated region (UTR).[6] *COL4A1* encodes collagen type IV alpha 1 chain. Collagen type IV is one of the components of the brain vascular basement membrane responsible for maintaining mechanical stability.[7] The causative variants in the *COL4A1* 3'UTR lead to upregulation of collagen type IV.[6] The recurrent ischemic episodes of PADMAL are likely to start in patients from their mid-thirties to mid-forties, with the radiological feature characterized by pontine multiple small infarctions and leukoencephalopathy.[6] The neuropathological findings for vessels in the brain and skin tissue show the accumulation of collagen type IV between the endothelial cells and vascular smooth muscle cells.[6,8] While loss-of-function effect associated with the variant in *COL4A1* can result in the dysfunction of vessels, including intracranial hemorrhage,[9] the occurrence of hemorrhage in PADMAL is relatively rare.

Although several cases of PADMAL have been reported worldwide, including Asia,[10-12] key signs for determining a PADMAL diagnosis have yet to be established. As a result, this situation makes it more difficult to diagnose young adult patients with undetermined cSVD as PADMAL. While certain risk factors of PADMAL have not been established yet, sporting activities with a high risk of head trauma or prolonged exercise are considered to be avoided for patients with *COL4A1/2* variants.[5] Therefore, if we can detect patients with PADMAL more precisely, we would be able to recognize higher risks of recurrent brain infarctions with them. Here, we present important radiological and neuropathological features of patients with PADMAL, which makes it possible to more accurately screen patients with PADMAL.

Materials and methods

Participants

First, we clinicoradiologically and genetically examined two patients (F1-IV-2 and F1-IV-6) with undetermined familial cSVD and five unaffected relatives in Family 1. Their family history and hemiparesis enabled us to make a diagnosis of familial cSVD.

Second, we then performed a retrospective cohort study that evaluated clinicoradiological features of the patients with juvenile cerebral vascular disorder (CVD) (n = 40; age of the onset between age 31 and 50 years) who were admitted to Hiroshima University Hospital from January 2011 to April 2021. We included consecutive patients who were diagnosed with acute brain infarctions based on the clinical onset and radiological findings within seven days from the onset.

Ethical consideration

This study was approved by the Ethics Committees of the participating institutions. Written informed consent was obtained from all participants who underwent genetic analysis or their legal representatives.

Neuroimaging

We clarified the radiological feature shared by two patients (F1-IV-2 and F1-IV-6) in Family 1 by assessing their findings on MRI. Subsequently, we then screened a cohort of CVD patients and selected patients exhibiting radiological features that were similar to those observed in F1-IV-2 and F1-IV-6. Patients in Family 1 and the CVD cohort were radiologically examined by either or both of CT and MRI. Sequences of MRI included at least diffusion weighted imaging, fluid attenuated inversion recovery (FLAIR), MR angiography (MRA) and

T2*. Two observers (M.K. and T.O.) consistently rated MR images of patients in Family 1 and the juvenile CVD cohort with their clinical information.

Whole exome sequencing

We performed whole exome sequencing (WES) in patients (F1-IV-2 and F1-IV-6) and their unaffected relative (F1-IV-1) in Family 1 using the Illumina platform (Illumina, San Diego, CA). Genomic DNA was extracted from peripheral blood leukocytes by using QuickGene-610L (Kurabo Industries Ltd., Osaka, Japan). Mapping to the human genome reference (GRCh37) was done using the Burrows–Wheeler alignment tool, with the removal of duplicate reads performed by Picard. Variant calls and annotation were done using GATK and Annovar.

Sanger sequencing

Sanger sequencing was performed by using 3130xl Genetic Analyzer (Thermo Fisher Scientific, Waltham, MA) in F1-III-14, F1-III-17, F1-III-18, F1-IV-3, F1-IV-7, F1-IV-9 and the patients selected from the cohort (F2-IV-8 and F3-III-2). Using this procedure, we were able to confirm the variant detected in WES. The forward and reverse primer sequences used in the polymerase chain reaction were 5'-AGGTCAATGAAGCAGGGTGT-3' and 5'-GCCATGTTTCTGACGTGCTG-3', respectively. The sequence for the primer used for the Sanger sequencing was 5'- TTTTAGGAAGCCTACGCCGT-3'.

Postmortem examination

The diagnosis for the deceased patient (F1-IV-2) in Family 1 was confirmed pathologically by a postmortem examination. Immediately after the postmortem examination, organs were fixed in 10% formalin and 7 μm-thick paraffin-embedded sections were stained with hematoxylin and eosin (HE) and Klüver–Barrera (KB) staining. Immunohistochemistry

was performed with rabbit polyclonal antibody against COL4A1 (1:100, SAB4300825, Sigma-Aldrich, St Louis, MO) and α-smooth muscle actin (α-SMA) (1:250, ab7817, Abcam, Cambridge, MA) through the use of a Ventana BenchMark GX automated slide staining system (Ventana Medical Systems, Tucson, AZ) in accordance with the instructions of the manufacturer.

Statistical analysis

We calculated a positive predictive value for the radiological feature shared among the Family 1 patients during the cohort screening. Fisher's exact test was performed by using R for assessing the correlation between the shared radiological features and clinical features. A value of $p < 0.05$ was considered significant.

Data availability

Protocols and other non-individual information are available on request.

Results

Clinical features

A pedigree chart of Family 1 is depicted in Fig. 1A, while Supplementary Table 1 presents the clinical features of the two examined patients (F1-IV-2 and F1-IV-6).

The first patient in Family 1 was F1-IV-2. She had hemiparesis on her right lower extremity at the age of 39 and was diagnosed with a brain infarction without any vascular risk factors. After the first episode, she had suffered from recurrent brain infarctions despite continuous administration of antiplatelets, and stepwise cognitive impairment was observed at 45 years of age. Her brain MRI showed bilateral diffuse ischemic lesions and bilateral WMH

(Fig. 2A). Her paresis gradually worsened, leading to a bedridden state before the age of 57 years (Supplementary Table 1). At the age of 57, her brain MRI showed bilateral cerebellar infarctions (Supplementary Fig. 3). The patient passed away at 59 years of age. The postmortem examination was performed at 13.5 hours after her death.

The second patient in Family 1 was F1-Ⅳ-7. At the age of 35, he had sudden hemiparesis and anesthesia in his right extremities and dysarthria, and MRI showed a brain infarction (Fig. 2B). He also suffered from recurrent infarctions despite continuous administration of antiplatelets. His MRI findings and intolerance of antiplatelets suggested that he could suffer from multiple sclerosis (MS). However, the examination of cerebrospinal fluid and the evaluation by contrast-enhanced MRI did not show any findings suggesting MS. While he showed only slight hemiparesis, deep tendon reflex in his extremities was exaggerated asymmetrically. Moreover, Chaddock reflex was present in his left foot suggesting a pyramidal sign.

F1-III-7, the father of F1-IV-6, had shown euphoria with a history of recurrent brain infarctions and died at the age of 62. Bilateral hyperreflexia and pyramidal sign were the shared clinical features found among the patients in Family 1.

Genetic analysis

We searched for the variants shared by F1-IV-2 and F1-IV-6 in WES, and detected six heterozygous variants. The shared variants included two intronic deletions in *GCM2*, one exonic single nucleotide variant (SNV) in *HECTD2*, one SNV in *COL4A1* 3'UTR, one intronic SNV in *COL4A2*, and one SNV in *ING1* 5'UTR. Among these genes, *COL4A1* 3'UTR was the only site reported to be causative of adult cSVD. All of the other variants were either benign

or not related to adult cSVD based on ClinVar (ncbi.nlm.nih.gov/clinvar/) and OMIM (ncbi.nlm.nih.gov/omim). The identified variant, *COL4A1*:c.*33T>A, with a combined annotation dependent depletion score of 13.85, was identical to the variant reported in the previous study of cSVD.[10] The variants in *COL4A1* 3'UTR have been reported to be causative of PADMAL,[6] and patients F1-IV-2 and F1-IV-6 were diagnosed with PADMAL. The same SNV in *COL4A1* 3'UTR was absent in F1-IV-1.

On the basis of the WES results, we confirmed the variant in the 3'UTR of *COL4A1* by Sanger sequencing using the genomic DNA of F1-IV-2 and F1-IV-6. We detected heterozygous *COL4A1*:c.*33T>A in these patients, while the variant was absent in the controls (Fig. 1D and E, Supplementary Fig. 1A).

Radiological features

F1-IV-2 and F1-IV-6 were examined by 1.5T MRI and had multiple small infarctions in both the pons and the subcortical hemispheric area (Fig. 2A and B). FLAIR showed the presence of white matter hyperintensities (WMH) in both patients, which were more broad and severe in F1-IV-2. No severe hemispheric microbleeds were seen by gradient echo T2 (T2*)-weighted images in both patients. MRA showed that there was no severe stenosis in depicted vessels including the anterior, middle and posterior cerebral arteries, internal carotid arteries, basilar artery and vertebral arteries in either of the patients (Supplementary Fig. 2A and B). The multiple small oval lesions in the pons were especially characteristic and shared by F1-IV-2 and F1-IV-6, while this feature was absent in F1-IV-1 (control). As the appearance of the pons that contained these characteristic small oval infarctions resembled raisin bread, we coined the name "raisin bread sign" for this unique radiological feature. The raisin bread sign was defined as containing at least two or more oval ischemic lesions, with distribution on the bilateral sides of the pons, except at the edges.

Postmortem pathological findings

We evaluated the clinicoradiological feature of one PADMAL patient (F1-IV-2) pathologically during a postmortem examination.

Brain weight was 1,160 g and the gross examination revealed atrophy of brainstem, and atherosclerosis of the basilar artery (Fig. 3 A and B). Oval ischemic lesions in the pons were observed at the locations identical to that of the raisin bread sign observed on the MRI (Fig. 3 C–E). Histopathological examination revealed hyalinized vessels and thickened media tunica of arterioles in the tissue spared from the ischemia (Fig. 3F), while the ischemic lesions did not show these features (Fig. 3G and H). Media tunica of arterioles, regardless of the presence of ischemic lesions, was positive for COL4A1 (Fig. 3I and L) and α-SMA (Fig. 3J and M) on immunohistochemistry, with accumulated COL4A1 only recognized in the thickened media tunica (Fig. 3K and L). Histopathological observation also revealed pyramidal tract atrophy in the pons, medulla oblongata and cervical spinal cord, including the corticospinal tract (Fig. 3D and E).

Screening for the raisin bread sign

Subsequently, we then screened the cohort of juvenile CVD patients at Hiroshima University Hospital for clinicoradiological features and selected patients found to have the raisin bread sign. Supplementary Table 2 presents the population characteristics of the cohort including the settings of radiological evaluation performed with these patients. In this cohort, four patients were evaluated only by CT and exhibited obvious infarctions in the cortex or basal ganglia without lesions in the pons. Three of them were diagnosed with "cardio-embolism" and had cardiac devices. The other one had non-bacterial thrombotic endocarditis caused by endometrial cancer and was diagnosed with "cancer-associated stroke". From this cohort, we identified two patients showing the raisin bread sign and stroke subtypes of both of them were

classified as "others undetermined". Although one CVD patient (F2-II-3) had a familial history of young-onset brain infarction, the other CVD patient (F3-II-2) did not. Fig.1 presents their pedigree charts. These patients also had characteristic small oval infarctions in the pons, and multiple small infarctions in the subcortical hemispheric area and WMH (Fig. 2C and D). Microbleeds and stenosis were not observed among these patients (Supplementary Fig. 2C and D). *COL4A1*:c.*33T>A was detected by Sanger sequencing using the genomic DNA of F2-II-3 and F3-II-2 (Supplementary Fig. 1B and C). Based on these results and clinicoradiological features, both patients were diagnosed with PADMAL. Therefore, these results suggest that the raisin bread sign has a high positive predictive value in detecting PADMAL. We also evaluated several clinical signs among patients with and without the raisin bread sign (Supplementary Table 3). Bilateral hyperreflexia was only observed in the group with the raisin bread sign.

Discussion

Previous studies have not precisely evaluated the diagnostic value of radiological features of PADMAL, with genetic analysis the only method used to diagnose PADMAL. Early diagnosis, however, is beneficial in predicting the prognosis and preventing excess administration of antiplatelets. In this study, by analyzing a family with *COL4A1* 3'UTR variants, we were able to determine that the pontine multiple small oval infarctions were a characteristic radiological feature of patients with PADMAL, with this radiological feature referred to as the raisin bread sign. We also were able to verify this radiological feature of PADMAL during a postmortem pathological examination. Subsequently, we then identified two patients among a cohort of young stroke patients who exhibited the raisin bread sign on MRI. Further evaluation confirmed that they harbored the heterozygous variants in *COL4A1*

3'UTR. The screening results for our juvenile CVD cohort demonstrated that this radiological feature was useful for the genetic diagnosis of PADMAL.

As described in a previous study, although PADMAL is radiologically characterized by pontine involvement with multiple infarcts, the detailed characteristics and specific shapes of the ischemic lesions have remained unclear.[6,11,13,14] Based on our current radiological analysis, we coined the name "raisin bread sign" for these pontine multiple small oval infarctions that were commonly observed among the patients in Family 1. During the postmortem examination of F1-IV-2, these small infarcts were pathologically confirmed in the pons, reflecting the distribution and shapes depicted as the raisin bread sign on MRI. The causative variant of PADMAL in the 3'UTR of *COL4A1* results in the accumulation of collagen type IV, which leads to fibrosis of the subendothelial space and lamina muscularis in the cerebral small arteries.[6,8] These pathological changes have been assumed to cause multiple infarctions, and as mentioned previously, thickened tunica media was observed in the postmortem examination in this study.[6,11,15] Interestingly, hyalinized vessels and thickened tunica media of arterioles were restricted in the area spared from ischemia. The infarctions were associated with small arteries that had tunica media of normal thickness, and there were no hyalinized vessels within the ischemic lesions. The distribution of hyalinized vessels was not consistent with that of the lacunar infarctions.[16,17] Although thickened arteriolar walls are also observed in ischemic lesions in cerebral autosomal dominant arteriopathy with subcortical infarcts and leukoencephalopathy (CADASIL),[17-19] the distribution of the small arteries with thickened media tunica in PADMAL was quite different from that observed in CADASIL. Furthermore, the pyramidal tract atrophy was obvious and intriguingly correlated with the clinical pyramidal signs observed in all patients. In this study, patients with PADMAL started to show the pyramidal sign during the early stages, and this clinical feature reflecting a pathological change may also be helpful in detecting patients with PADMAL among cSVD patients.

Although WMH was also observed among the patients with PADMAL, similar to the other adult-onset genetic leukoencephalopathies,[20] we tried to establish a radiological sign that was more specific to PADMAL. On the basis of the correlation between the raisin bread sign and the pathological findings that were confirmed in the postmortem examination, we attempted to use this radiological sign during the screening of PADMAL patients that were evaluated among young patients in a CVD cohort. As well as finding involvement of the anterior temporal pole on MRI in CADASIL that helps facilitate the genetic diagnosis,[3-5] the results of our study also suggest that the raisin bread sign is an indicative sign of PADMAL. Previous studies also reported pontine MRI findings from ten genetically-confirmed PADMAL patients.[6, 11, 13] All their MRI findings presented several oval lesions in pons, which we considered as the raisin bread sign. Thus, the raisin bread sign allows more efficient selection of the candidates for genetic analysis of *COL4A1* 3'UTR. This sign is also effective even when the patient is sporadic, indicating that an absence of family history is not always sufficient for excluding the possibility of PADMAL. One of the limitations of our study was that we did not perform genetic analysis among patients without the raisin bread sign, and thus, precise estimation of the sensitivity and specificity was difficult. In addition, while the patients examined in this study all harbored the same variant in *COL4A1* 3'UTR, the number of multiple infarctions and severity of leukoencephalopathy varied among these patients and was not correlated with the age at the first stroke episode. Therefore, there may be another factor affecting the burden of lesions of PADMAL besides the location of variants.

In a previous report, a variant in a location other than *COL4A1* 3'UTR was identified to be causative of hereditary multi-infarct dementia of the Swedish type, which was characterized by cognitive impairment, depressive illness, and behavioral symptoms, including mood changes.[21,22] These symptoms can also be observed among patients with PADMAL,[6] with two of our patients exhibiting cognitive dysfunction and mood disturbance as the disease

progressed. The phenotypes related to variants in *COL4A1* 3'UTR may be varied as well as those caused by the variants within the coding region of *COL4A1*.[23]

In the present study, we detected an important radiological sign of PADMAL, which we refer to as the raisin bread sign, that can be used as a factor in helping decide on whether to perform genetic analysis for *COL4A1* 3'UTR in patients whose family histories are unavailable. Moreover, the correlation between radiological and neuropathological features recognized in our study could potentially provide important information that can be used in the detection of the detailed mechanism of PADMAL in the future.

Acknowledgements

We thank all of the enrolled patients and their families for their participation, which allowed for the data collection and analysis in this study. We thank Eiko Nakajima (Department of Epidemiology, Research Institute for Radiation Biology and Medicine, Hiroshima University), Yasuko Furuno, Miwako Sasanishi (Department of Clinical Neuroscience and Therapeutics, Hiroshima University Graduate School of Biomedical and Health Sciences), Hiroki Fujisawa, Arisa Kan (Department of Diagnostic Pathology, National Hospital Organization Kure Medical Center and Chugoku Cancer Center) for their excellent technical assistance.

Funding

This work was supported in part by grants from Grants-in-Aid for Scientific Research from Japan Society for the Promotion of Science (JSPS) and grants from Takeda Science Foundation and Tsuchiya Memorial Medical Foundation to T.K. T.N. received a Grant-in-Aid for

Scientific Research (20K16579). S.A. received a grant from JSPS KAKENHI (Grant 21K10210).

Competing interests

The authors report no competing interests.

Supplementary material

Supplementary material is available at *Brain* online.

References

1. Fang C, Magaki SD, Kim RC, et al. Arteriolar neuropathology in cerebral microvascular disease. *Neuropathol Appl Neurobiol.* 2023;49(1):e12875. doi:10.1111/nan.12875

2. Wardlaw JM, Smith C, Dichgans M. Mechanisms of sporadic cerebral small vessel disease: insights from neuroimaging. *Lancet Neurol.* 2013;12:483-497

3. Marcus HS, Martin RJ, Simpson MA, et al. Diagnostic strategies in CADASIL. *Neurology* 2002;59:1134-1138

4. Eswaradass PV, Ramasamy B, Kalidoss R, Gnanashanmugham G. Anterior temporal lobe involvement: Useful magnetic resonance imaging sign to diagnose Cerebral Autosomal Dominant Arteriopathy with Subcortical Infarcts and Leukoencephalopathy. *J Neurosci Rural Pract.* doi:10.4103/0976-3147.165391

5. Mancuso M, Arnold M, Bersano A, et al. Monogenic cerebral small-vessel diseases: diagnosis and therapy. Consensus recommendations of the European Academy of Neurology. *Eur J Neurol.* 2020;27: 909-927. doi:10.1111/ene.14183.

6. Verdura E, Hervé D, Bergametti F, et al. Disruption of a miR-29 binding site leading to COL4A1 upregulation causes pontine autosomal dominant microangiopathy with leukoencephalopathy. *Ann Neurol* 2016;80:741-753

7. Timpl R. Macromolecular organization of basement membranes. *Curr Opin Cell Biol* 1996;8:618-624

8. Craggs LJL, Hagel C, Kuhlenbaeumer G, et al. Quantitative vascular pathology and phenotyping familial and sporadic cerebral small vessel diseases. *Brain Pathology* 2013;23:547-557

9. Lanfranconi S, Markus HS. COL4A1 mutations as a monogenic cause of cerebral small vessel disease: A systematic review. *Stroke* 2010;41:e513-e518

10. Sakai N, Uemura M, Kato T, et al. Hemorrhagic cerebral small vessel disease caused by a novel mutation in 3'UTR of collagen type IV alpha 1. *Neurol Genet* 2020;6:e383. doi:10.1212/NXG.0000000000000383

11. Zhao YY, Duan RN, Ji L, et al. Cervical Spinal Involvement in a Chinese Pedigree With Pontine Autosomal Dominant Microangiopathy and Leukoencephalopathy Caused by a 3′ Untranslated Region Mutation of COL4A1 Gene. *Stroke* 2019;50:00-00. doi:10.1161/ STROKEAHA.119.024875.

12. Li Q, Wang C, Li W, et al. A Novel Mutation in COL4A1 Gene in a Chinese Family with Pontine Autosomal Dominant Microangiopathy and Leukoencephalopathy. *Transl Stroke Res.* 2022;13(2): 238-244. doi:10.1007/s12975-021-00926-0

13. Grobe-Einsler M, Urbach H, Paus S. Recurrent Pontine Strokes in a Young Male. *J Stroke Cerebrovasc Dis.* 2020;29(12):105386. doi:10.1016/j.jstrokecerebrovasdis.2020.105386.

14. Ding XQ, Hagel C, Ringelstein B, et al. MRI Features of Pontine Autosomal Dominant Microangiopathy and Leukoencephalopathy (PADMAL). *J Neuroimaging* 2010;20:134-140.

15. Hagel C, Groden C, Niemeyer R, et al. Subcortical angiopathic encephalopathy in a German kindred suggests an autosomal dominant disorder distinct from CADASIL. *Acta Neuropathol*. 2004;108:231-240

16. Yaghi S, Raz E, Yang D, et al. Lacunar stroke: mechanisms and therapeutic implications. *J Neurol Neurosurg Psychiatry.* 2021;92:823-830. doi:10.1136/jnnp-2021-326308.

17. Craggs LJ, Yamamoto Y, Deramecourt V, et al. Microvascular pathology and morphometrics of sporadic and hereditary small vessel diseases of the brain. *Brain Pathol.* 2014;24:5:495-509. doi:10.1111/bpa.12177.

18. Miao Q, Paloneva T, Tuominen S, et al. Fibrosis and Stenosis of the Long Penetrating Cerebral Arteries: the Cause of the White Matter Pathology in Cerebral Autosomal Dominant Arteriopathy with Subcortical Infarcts and Leukoencephalopathy. *Brain Pathol.* 2004;14:358-364.

19. Okeda R, Arima K, Kawai M. Arterial Changes in Cerebral Autosomal Dominant Arteriopathy With Subcortical Infarcts and Leukoencephalopathy (CADASIL) in Relation to Pathogenesis of Diffuse Myelin Loss of Cerebral White Matter Examination of Cerebral Medullary Arteries by Reconstruction of Serial Sections of an Autopsy Case. *Stroke* 2002;33:2565-2569.

20. Ayrignac X, Carra-Dalliere C, Menjot de Champfleur N, et al. Adult-onset genetic leukoencephalopathies: a MRI pattern-based approach in a comprehensive study of 154 patients. *Brain.* 2015;138:284-292. doi:10.1093/brain/awu353.

21. Low WC, Junna M, Börjesson-Hanson A, et al. Hereditary multi-infarct dementia of the Swedish type is a novel disorder different from NOTCH3 causing CADASIL. *Brain.* 2007;130:357-367. doi:10.1093/brain/awl360.

22. Siitonen M, Börjesson-Hanson A, Pöyhönen M, et al. Multi-infarct dementia of Swedish type is caused by a 3'UTR mutation of COL4A1. *Brain.* 2017;140:5:e29. doi:10.1093/brain/awx062.

23. Lanfranconi S, Markus HS. COL4A1 mutations as a monogenic cause of cerebral small vessel disease: A systematic review. *Stroke* 2010;41:e513-e518.

Figure legends

Figure1 The pedigree charts of three PADMAL families (Family 1–3) and the identified variant in *COL4A1* 3' untranslated region (UTR)

(**A–C**) Square symbols indicate men and round symbols indicate women. Closed symbols indicate affected individuals proven by clinical histories or MRI. Diagonal lines indicate deceased individuals. Open symbols indicate individuals without PADMAL proven clinically or radiologically. Arrows indicate probands. The pedigree charts of F1 (**A**) and F2 (**B**) show autosomal dominant inheritance pattern while F3 (**C**) does not. (**D**) Sanger sequencing was performed with the proband (F1-IV) in F1. The heterozygous variant of *COL4A1* located in c.*33T>A was identified, which is indicated by an arrowhead. (**E**) The healthy control in F1 (F1-IV-1) showed no variant in *COL4A1* 3'UTR in Sanger sequencing.

Figure2 MRI features of the probands in Family 1–3

(**A–D**) MRI scan was performed using the genetically proven probands at 1.5 T in Family 1 and at 3 T in Family 2 and 3. The examination was performed nine years after the onset for F1-IV-2 (**A**), seven years after the onset for F1-IV-6 (**B**), eight years after the onset for F2-II-3 (**C**), and 12 years after the onset for F3-II-2 (**D**). T1-weighted images (T1WI) show low intensity areas located in the pons and white matter in all four cases. The pontine atrophy was observed in the autopsy case (F1-IV-2). Multiple infarctions were observed in the pons on fluid attenuated inversion recovery (FLAIR), and corresponded to the low intensity areas depicted on T1WI. Every patient showed at least one oval shape lesion in the pons. Bilateral white matter hyperintensity was also observed in all cases.

Figure3 Histopathology in F1-IV-3

(**A, B**) Gross finding of the brain of F1-IV-2. Atrophies of frontotemporal lobes and brainstem, and the atherosclerosis of the basilar artery were observed. (**C**) The focused image of the pons on FLAIR. (**D, E**) Hematoxylin and eosin (HE) staining (**D**) and Klüver–Barrera staining (**E**) sections of the pons showed multiple infarctions and existing lesions revealed by MRI. (**F**) Hyalinized vessels in the non-ischemic lesions had thickened media tunica. (**G**) The pontine ischemic lesions did not include vessels with thick media tunica. (**H–J**) Vessels in ischemic lesions (**H**) showed immunopositivity of COL4A1 (**I**) and α-SMA (**J**) around the vessels. (**K–M**) Vessels in the non-ischemic areas (**K**) was hyalinized with thick media tunica, which were immunopositive for COL4A1 (**L**) and α-SMA (**M**).

Scale bars: (**D, E**) 1 mm, (**F, G**) 200 μm, (**H–J, L, M**) 20 μm, (**K**) 100 μm

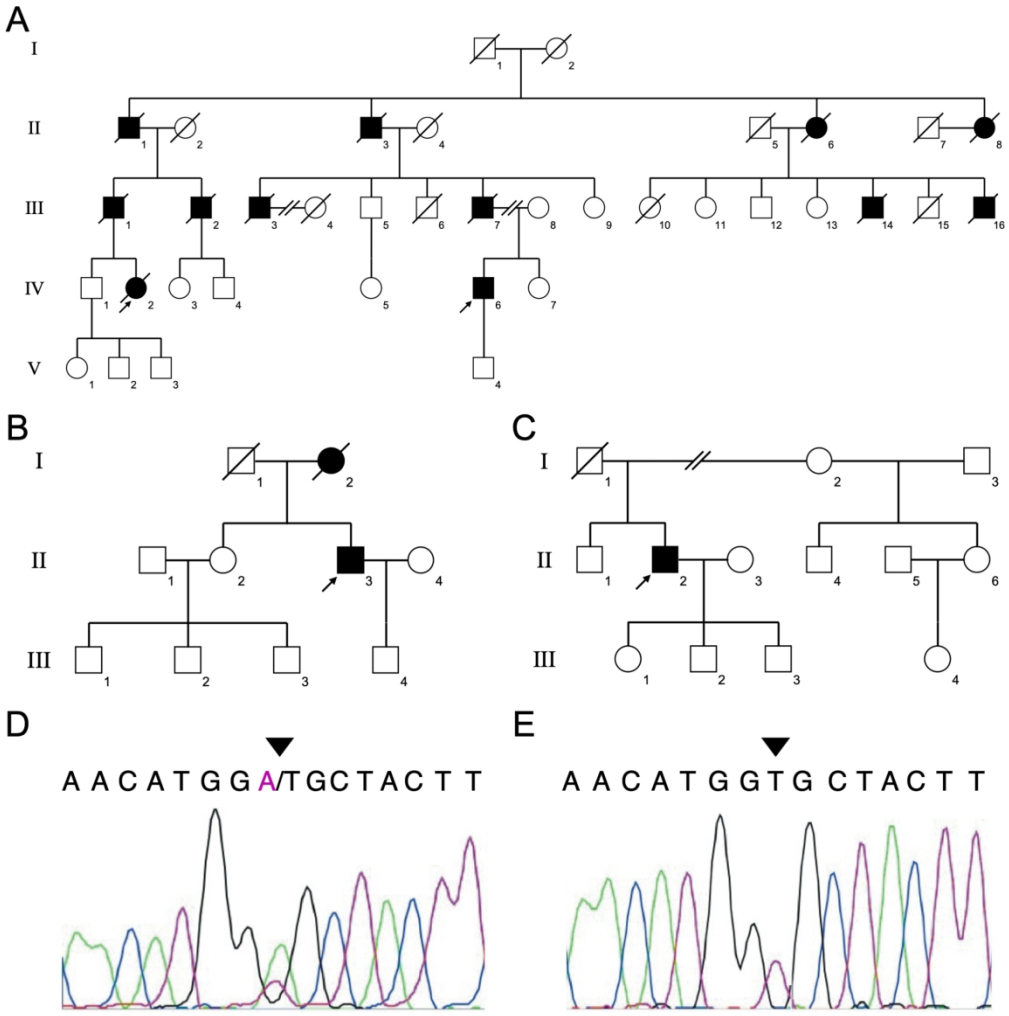

Figure1 The pedigree charts of three PADMAL families (Family 1–3) and the identified variant in COL4A1 3′ untranslated region (UTR)
(A–C) Square symbols indicate men and round symbols indicate women. Closed symbols indicate affected individuals proven by clinical histories or MRI. Diagonal lines indicate deceased individuals. Open symbols indicate individuals without PADMAL proven clinically or radiologically. Arrows indicate probands. The pedigree charts of F1 (A) and F2 (B) show autosomal dominant inheritance pattern while F3 (C) does not. (D) Sanger sequencing was performed with the proband (F1-IV) in F1. The heterozygous variant of COL4A1 located in c.*33T>A was identified, which is indicated by an arrowhead. (E) The healthy control in F1 (F1-IV-1) showed no variant in COL4A1 3′UTR in Sanger sequencing.

215x217mm (300 x 300 DPI)

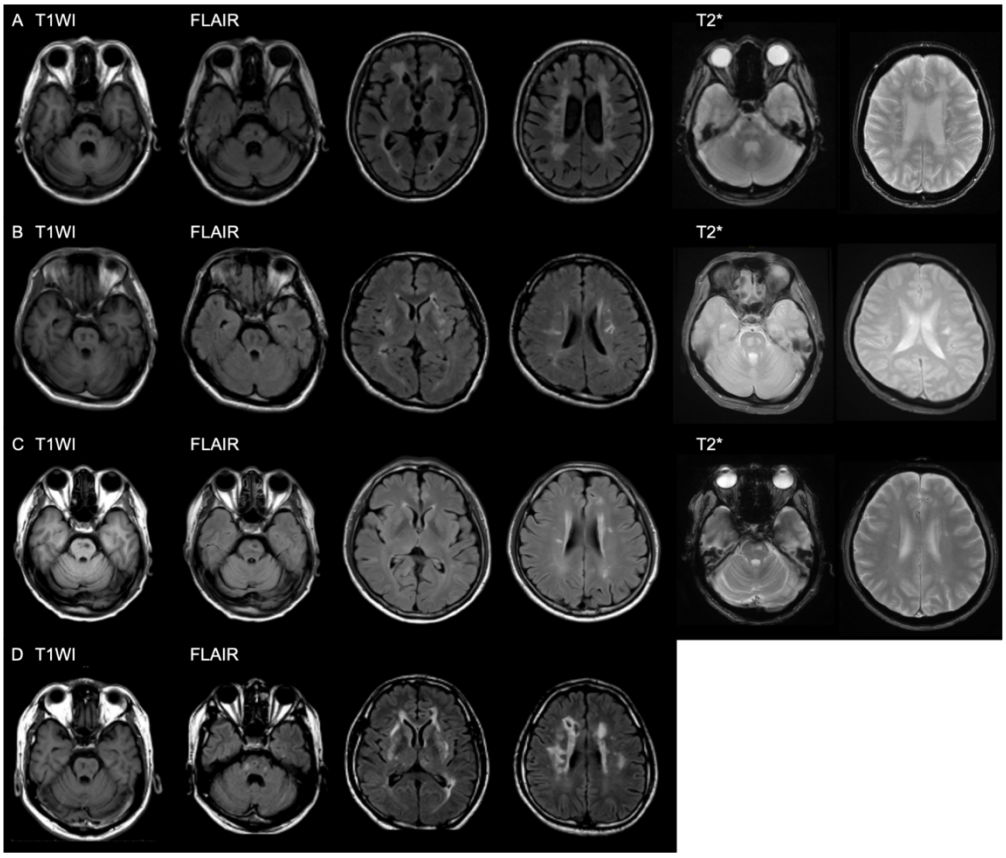

Figure2 MRI features of the probands in Family 1–3
(A–D) MRI scan was performed using the genetically proven probands at 1.5 T in Family 1 and at 3 T in Family 2 and 3. The examination was performed nine years after the onset for F1-IV-2 (A), seven years after the onset for F1-IV-6 (B), eight years after the onset for F2-II-3 (C), and 12 years after the onset for F3-II-2 (D). T1-weighted images (T1WI) show low intensity areas located in the pons and white matter in all four cases. The pontine atrophy was observed in the autopsy case (F1-IV-2). Multiple infarctions were observed in the pons on fluid attenuated inversion recovery (FLAIR), and corresponded to the low intensity areas depicted on T1WI. Every patient showed at least one oval shape lesion in the pons. Bilateral white matter hyperintensity was also observed in all cases.

184x157mm (300 x 300 DPI)

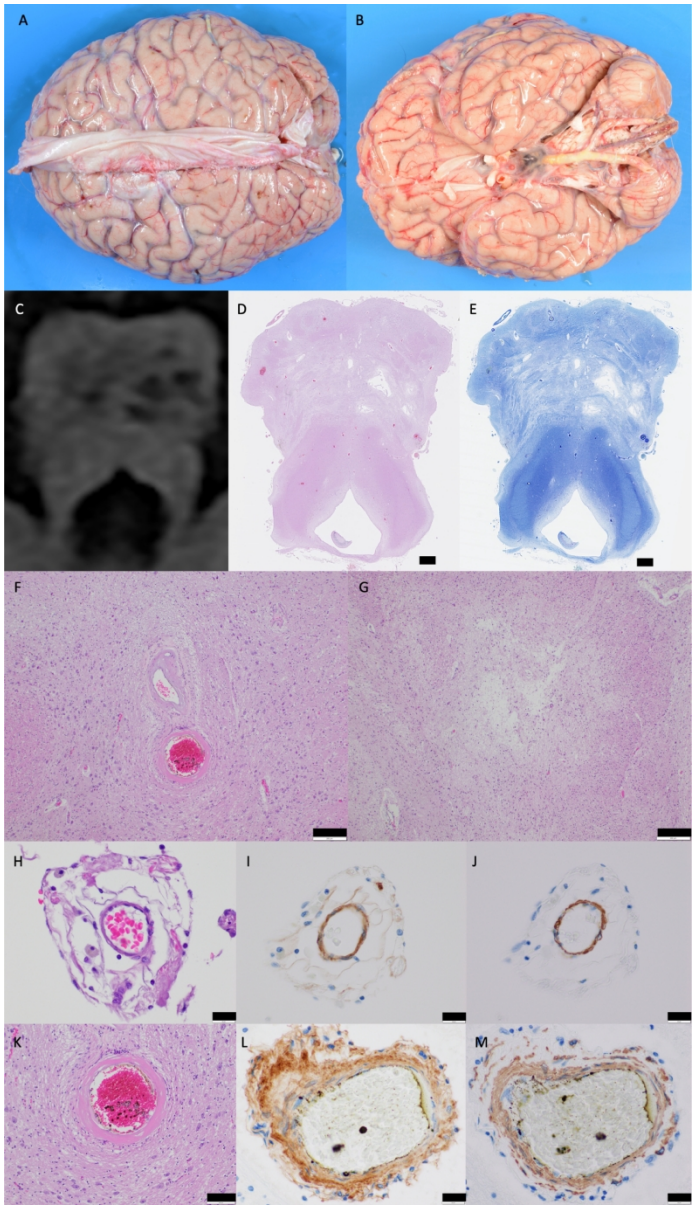

Figure3 Histopathology in F1-IV-3
(A, B) Gross finding of the brain of F1-IV-2. Atrophies of frontotemporal lobes and brainstem, and the atherosclerosis of the basilar artery were observed. (C) The focused image of the pons on FLAIR. (D, E) Hematoxylin and eosin (HE) staining (D) and Klüver–Barrera staining (E) sections of the pons showed multiple infarctions and existing lesions revealed by MRI. (F) Hyalinized vessels in the non-ischemic lesions had thickened media tunica. (G) The pontine ischemic lesions did not include vessels with thick media tunica. (H–J) Vessels in ischemic lesions (H) showed immunopositivity of COL4A1 (I) and α-SMA (J) around the vessels. (K–M) Vessels in the non-ischemic areas (K) was hyalinized with thick media tunica, which were immunopositive for COL4A1 (L) and α-SMA (M).
Scale bars: (D, E) 1 mm, (F, G) 200 μm, (H–J, L, M) 20 μm, (K) 100 μm

160x278mm (300 x 300 DPI)

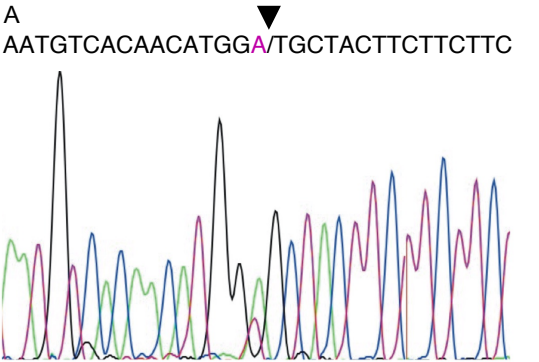
A
AATGTCACAACATGGA/TGCTACTTCTTCTTC

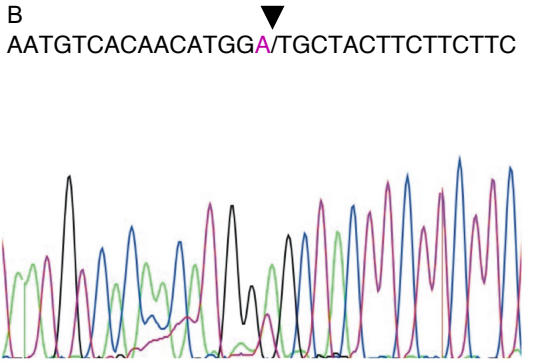
B
AATGTCACAACATGGA/TGCTACTTCTTCTTC

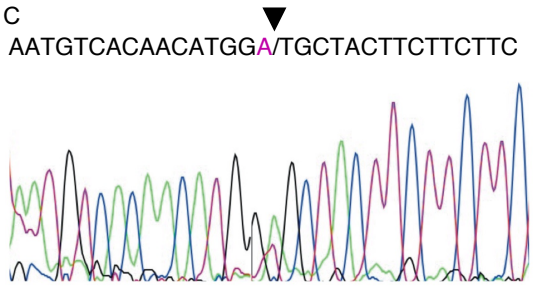
C
AATGTCACAACATGGA/TGCTACTTCTTCTTC

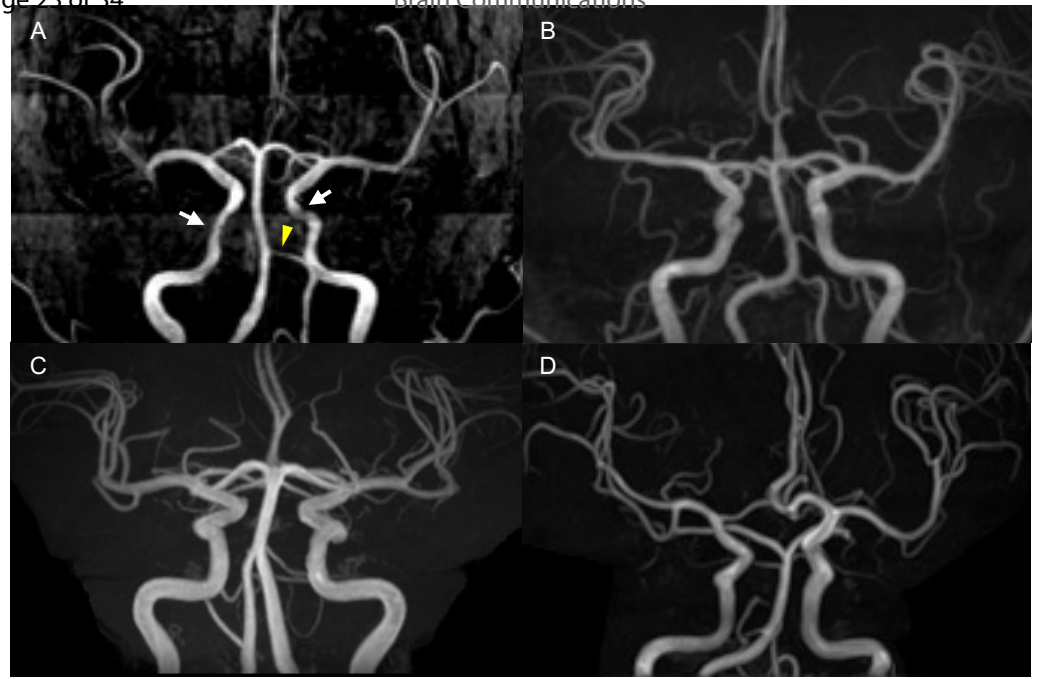
A
B
C
D

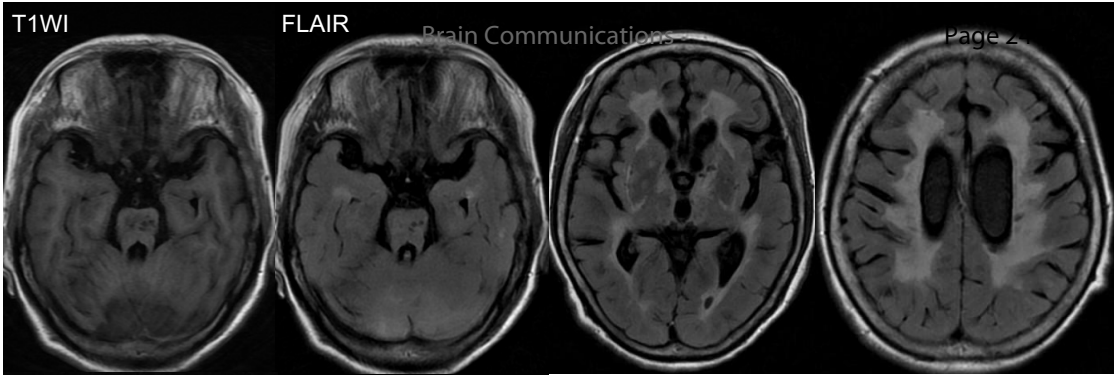
T1WI
FLAIR

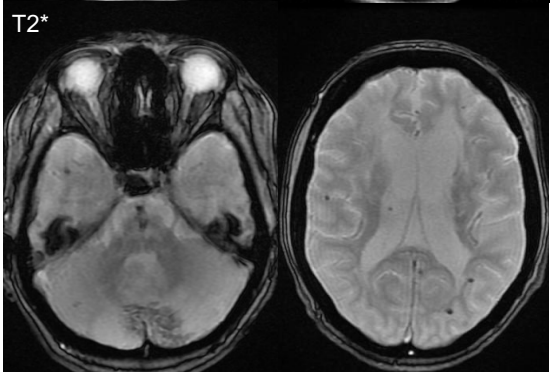
T2*

Supplementary Fig. 1 Results of Sanger sequencing

(**A–C**) Result of the Sanger sequencing performed in F1-IV-6 (**A**), F2-II-3 (**B**), and F3-II-2 (**C**) showed the heterozygous variant of collagen type IV alpha chain (*COL4A1*) located in c.*33T>A, which was identical to F1-IV-2.

Supplementary Fig. 2 Magnetic resonance angiography

(**A**) Magnetic resonance angiography (MRA) showed slight stenosis in both carotid arteries (arrows) and the left vertebral artery (arrowhead) in F1-IV-2. (**B–D**) No stenosis was observed in F1-IV-6, F2-II-3 and F3-II-2 on MRA.

Supplementary Fig. 3 MRI performed during the early period in F1-IV-2

MRI was performed at 17 years after F1-IV-2 onset. Multiple bilateral infarctions and WMH were observed in the pons on FLAIR. Although low intensity areas were observed on T1WI that corresponded to the multiple infarctions shown on FLAIR, pontine atrophy was not obvious.

Supplementary Table 1 Clinical features of the patients with PADMAL

Patient	Age at 1st stroke (y)	mRS (age, y)	Paresis	Bilateral hyperreflexia	Foot clonus	Cognitive impairment and/or mood disturbance
F1-IV-2	39	5 (57)	Hemiparesis in right extremities	+	−	+
F1-IV-6	35	1 (41)	Mild paresis in left plantar flexor and dorsiflexor (MMT 4)	+	+	−
F2-II-3	40	2 (48)	Mild paresis in right extremities (Barré's sign and Mingazzini sign are positive.)	+	+ (pseudo-clonus)	−
F3-II-2	36	3(49)	Mild paresis in left upper extremity (Barré's sign is positive.)	+	+ (pseudo-clonus)	+

mRS, modified Rankin scale; MMT, manual muscle testing

Supplementary Table 2 Characteristics of the cohort of juvenile CVD patients

Number of the patients	40
Age at onset, mean, y (SD)	43.3 (5.3)
Female, n (%)	9 (23.1)
Stroke subtype	
Large artery atherosclerosis, n (%)	3 (7.7)
Small vessel occlusion, n (%)	2 (5.1)
Cardio-embolism, n (%)	5 (12.8)
Cancer-associated stroke, n (%)	4 (10.3)
Cerebral artery dissection, n (%)	9 (23.1)
Others undetermined, n (%)	17 (43.6)
Radiological evaluation	
3T MRI, n (%)	32 (80)
1.5T MRI, n (%)	16 (40)
CT-only, n (%)	4 (10)
Patients with pontine lesions, n (%)	8 (20.5)
Raisin bread sign, n (%)	2 (5.1)

CVD, cerebral vessel disease; SD, standard deviation; CT, computed tomography

Supplementary Table 3 Clinical features of juvenile CVD patients with or without raisin bread sign

	Raisin bread sign positive (n = 2)	**Raisin bread sign negative (n = 38)**	
Hyperreflexia	2	6	$p = 0.1014$
Bilateral hyperreflexia	2	0	$p = 0.003623$
Paresis	2	17	$p = 0.2192$
Mild paresis (Barré's sign, Mingazzini sign or Wartenberg's sign with MMT 4–5)	2	5	$p = 0.05172$
Cognitive impairment or higher brain dysfunction	1	10	$p = 0.4899$
Mood disturbance	1	8	$p = 0.4038$

MMT, manual muscle testing

Family with Pontine Autosomal Dominant Microangiopathy And Leukoencephalopathy

Radiological feature

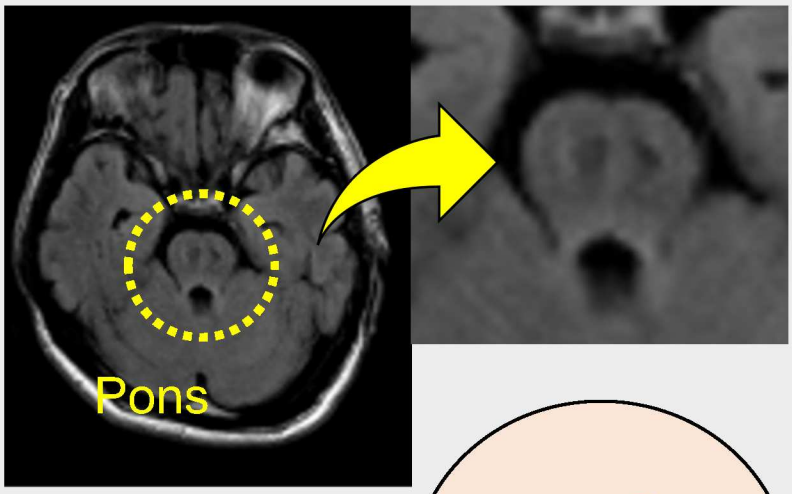

Variant in *COL4A1* 3'UTR

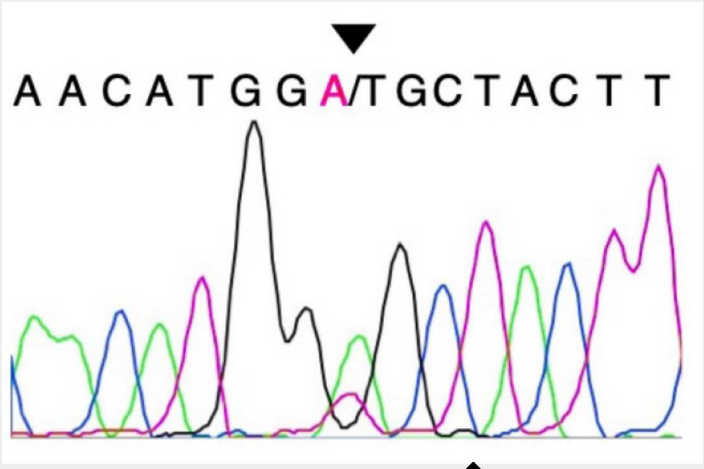

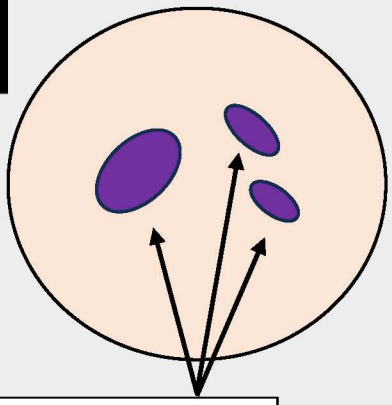

Multiple oval small infarctions
= **Raisin bread sign**

High positive predictive value

Juvenile cerebral vascular disorder cohort

Abbreviated Summary

Kikumoto *et al*. detected a characteristic radiological feature of pontine autosomal dominant angiopathy and leukoencephalopathy, which enables more accurate evaluations of patients with undetermined juvenile cerebral vascular disorder. This feature is multiple oval small infarctions in the pons resembling raisin bread, for which they coined the name "raisin bread sign".

STROBE statement: Reporting guidelines checklist for cohort, case-control and cross-sectional studies

SECTION	ITEM NUMBER	CHECKLIST ITEM	REPORTED ON PAGE NUMBER:
TITLE AND ABSTRACT			
	1a	Indicate the study's design with a commonly used term in the title or the abstract	1
	1b	Provide in the abstract an informative and balanced summary of what was done and what was found	1
INTRODUCTION			
Background and objectives	2	Explain the scientific background and rationale for the investigation being reported	3
	3	State specific objectives, including any pre-specified hypotheses	3
METHODS			
Study design	4	Present key elements of study design early in the paper	3-5
Setting	5	Describe the setting, locations, and relevant dates, including periods of recruitment, exposure, follow-up, and data collection	3-4
Participants	6a	Cohort study—Give the eligibility criteria, and the sources and methods of selection of participants. Describe methods of follow-up Case-control study—Give the eligibility criteria, and the sources and methods of case ascertainment and control selection. Give the rationale for the choice of cases and controls Cross-sectional study—Give the eligibility criteria, and the sources and methods of selection of participants	3-4
	6b	Cohort study—For matched studies, give matching criteria and number of exposed and unexposed Case-control study—For matched studies, give matching criteria and the number of controls per case Variables	None
Variables	7	Clearly define all outcomes, exposures, predictors, potential confounders, and effect modifiers. Give diagnostic criteria, if applicable	4-5

SECTION	ITEM NUMBER	CHECKLIST ITEM	REPORTED ON PAGE NUMBER:
Data sources/measurements	8*	For each variable of interest, give sources of data and details of methods of assessment (measurement). Describe comparability of assessment methods if there is more than one group.	4-5
Bias	9	Describe any efforts to address potential sources of bias.	3-5
Study size	10	Explain how the study size was arrived at	3-4
Quantitative variables	11	Explain how quantitative variables were handled in the analyses. If applicable, describe which groupings were chosen and why .	5
Statistical methods	12a	Describe all statistical methods, including those used to control for confounding	5
	12b	Describe any methods used to examine subgroups and interactions	5
	12c	Explain how missing data were addressed	3-5
	12d	Cohort study—If applicable, explain how loss to follow-up was addressed Case-control study—If applicable, explain how matching of cases and controls was addressed Cross-sectional study—If applicable, describe analytical methods taking account of sampling strategy	3-5
	12e	Describe any sensitivity analyses	5
RESULTS			
Participants	13a	Report numbers of individuals at each stage of study—eg numbers potentially eligible, examined for eligibility, confirmed eligible, included in the study, completing follow-up, and analysed	6-9
	13b	Give reasons for non-participation at each stage	6-9
	13c	Consider use of a flow diagram	None
Descriptive Data	14a	Give characteristics of study participants (eg demographic, clinical, social) and information on exposures and potential confounders	**6-9**
	14b	Indicate number of participants with missing data for each variable of interest	6-9
	14c	Cohort study—Summarise follow-up time (eg, average and total amount)	6-9
Outcome Data	15*	Cohort study—Report numbers of outcome events or summary measures over time	6-9

SECTION	ITEM NUMBER	CHECKLIST ITEM	REPORTED ON PAGE NUMBER:
		Case-control study—Report numbers in each exposure category, or summary measures of exposure Cross-sectional study—Report numbers of outcome events or summary measures	
Main Results	16a	Give unadjusted estimates and, if applicable, confounder-adjusted estimates and their precision (e.g. 95% confidence interval). Make clear which confounders were adjusted for and why they were included	6-9
	16b	Report category boundaries when continuous variables were categorized	None
	16c	If relevant, consider translating estimates of relative risk into absolute risk for a meaningful time period	None
	16d	Report results of any adjustments for multiple comparisons	8-9
Other Analyses	17a	Report other analyses done—e.g. analyses of subgroups and interactions, and sensitivity analyses	None
	17b	If numerous genetic exposures (genetic variants) were examined, summarize results from all analyses undertaken	6
	17c	If detailed results are available elsewhere, state how they can be accessed	None
DISCUSSION			
Key Results	18	Summarise key results with reference to study objectives	9
Limitations	19	Discuss limitations of the study, taking into account sources of potential bias or imprecision. Discuss both direction and magnitude of any potential bias	11
Interpretation	20	Give a cautious overall interpretation of results considering objectives, limitations, multiplicity of analyses, results from similar studies, and other relevant evidence	9-11
Generalisability	21	Discuss the generalisability (external validity) of the study results Other information	11
FUNDING			
	22	Give the source of funding and the role of the funders for the present study and, if applicable, for the original study on which the present article is based	12

*Give information separately for cases and controls in case-control studies and, if applicable, for exposed and unexposed groups in cohort and cross-sectional studies.